Supplementary Material

1. Methods

1.1 Radiocarbon chronology

Samples for radiocarbon dating from core NGHP-16A were disaggregated using distilled water and then sieved. Mixed planktonic foraminifera from the >250μm size fraction were picked first, and supplemented by tests from the >150μm size fraction when necessary. Radiocarbon measurements were performed at the National Ocean Sciences Accelerator Mass Spectrometry Facility (NOSAMS) in Woods Hole, MA, USA. Radiocarbon ages were converted to calendar ages using the CALIB 6.0 program [*Stuiver and Reimer,* 1993] and the Marine09 calibration curve [*Reimer et al.*, 2009]. Available reservoir estimates for the Bay of Bengal surface waters are not substantially different than the standard marine reservoir correction [*Dutta et al.*, 2001; *Southon et al.*, 2002], which we used to calibrate our data. Ages for samples between calibrated dates were obtained by linear interpolation. Results are shown in Supplementary Table 1 and Supplementary Figure 1.

1.2 Planktonic foraminifera oxygen isotopes

Stable isotope analysis of oxygen were performed on planktonic foraminifera *Globigerinoides ruber* (white) from the first 5.0 meters of core NGHP-16A at an average sampling resolution of 3 samples per century. Sediment samples of 10 cm^3 were wet-washed in a 63 μm sieve and picked foraminifera were washed and sonicated in distilled water before processing. All samples contained between 8-10 tests from the >150 μm fraction and weighed between 100-150 μg. Samples were processed using a VG Prism Mass Spectrometer at NOSAMS. Analytical

reproducibility as determined from replicate measurements on carbonate standard NBS-19 is better than 0.1‰.

1.3 Plant Wax Lipid Carbon Isotopes

Compound-specific carbon isotope analyses of *n*-alkanoic acids were performed on samples from the upper 8.0 meters of core NGHP-16A at a sampling resolution of 20 cm corresponding to an average sampling interval of 220 years (from ~440 years near the bottom of the core to ~ 125 years near the top of the core). Lipid organic matter was extracted from 10-12 grams of the freeze-dried sediment samples using a dichloromethane (DCM):methanol (MeOH) solution(9:1) in a CEM Microwave Accelerated Reaction System (MARS). Concentrated lipid extract was saponified with 0.5N KOH in methanol solution. Liquid/liquid extraction of the neutral fraction was done using pure hexane. Then the pH was adjusted to 2 by addition of HCl and liquid/liquid extraction of the acid fraction was performed using hexane:DCM (4:1). Lipids in the acid fraction, including leaf wax *n*-alkanoic acids, were methylated using HCl 5% in MeOH (70 ^{o}C for 12 hours). The resulting fatty acid methylesters (FAMEs) were extracted using hexane:DCM (4:1), then dried with anhydrous sodium sulfate, and then purified via silica gel chromatography. A FAMEs standard C_{13} – C_{24} was added to each sample sequence prior to analysis by gas chromatography (GC). All samples were initially analyzed by GC using an HP 5890 Series II GC equipped with flame ionization detector (FID). Isotope ratio monitoring GC–MS (GC/irMS) was used to determine $\delta^{13}C$ values of FAMEs. Measurements were performed on a Finnigan Delta^{Plus} stable isotope mass spectrometer attached to an HP 6890 GC (DB5-MS column) and Finnigan GC combustion III interface. All analyses were performed in triplicate. $\delta^{13}C$ values were determined relative to a reference gas (CO_2) of known isotopic composition, introduced in pulses

during each run. GC/irMS accuracy and precision are both better than 0.3‰. The results were corrected for the $\delta^{13}C$ composition of the methyl derivative (MeOH -39.56‰ ±0.2‰, measured at NOSAMS) based on isotopic mass balance in order to derive $\delta^{13}C$ values for the original *n*-alkanoic acids.

2. Geographical features of the Indian peninsula

The Indian peninsula is bordered by the Arabian Sea to the west, the Bay of Bengal to the east, the Indian Ocean to the south and the Tibetan plateau on the north (Supplementary Fig. 2). Important geographic features include: the Thar dessert to the northeast, the Indo-Gangetic Plain to the south of the Himalayas, which lies between the Indus and Ganga (Ganges) rivers, and the Deccan Plateau, a large igneous province consisting of multiple layers of flood basalts; the coastal mountain range of Sahyadri (Western Ghats) along the western coast, and the Eastern Ghats range along the eastern coast of the peninsula [*Washington,* 1922]. The Godavari Basin covers an area of 312,812 km^2, representing about 12% of the area of continental India (see fig.1b). The river headwaters lie on the northern end of the Western Ghats at an elevation of 920 m. However the mean elevation of the basin is estimated at 420 m [*Bikshamaiah and Subramanian*, 1980].

3. Hydroclimatology of the Indian peninsula and Bay of Bengal

The Indian peninsula and the Bay of Bengal exhibit pronounced seasonality with marked wet and dry seasons. In June through September precipitation is brought in by the moist southwest winds. The Western Ghats affects the precipitation pattern over peninsular India. Monsoonal rains in western India fall preferentially on the strip of land between the coast and the Ghats. Consequently the region located inland of the Ghats receives less precipitation and is semi-arid

to arid because of this particular orography [*Gunnell et al.,* 2007].

The Western Ghats also form the drainage divide for peninsular India: main rivers within the Deccan plateau have their headwaters in the Western Ghats and flow east towards the Bay of Bengal. The Godavari River and its tributaries, drain most of the northern portion of the plateau, The Krishna River and its tributaries, drain the central portion of the plateau, and the southernmost portion of the plateau is drained by the Kaveri (Cauveri) River. There is a large seasonal variability in freshwater flux, with most of the total river runoff coming in during the summer monsoon. As a result, there is a strong freshening of surface waters in the coastal regions of the Bay of Bengal during/after the summer monsoon. The large impact of river discharge produces salinity changes on the order of 6 psu between summer and winter [*Antonov et al.*, 2006]. Modern salinity patterns indicate that the strongest salinity variations in the western Bay of Bengal occur in front of the Godavari mouths (Supplementary Fig. 3). A persistent sediment plume extends ~300 km offshore the Godavari river mouth [Sridhar et al., 2008]. During the Holocene, the Godavari delivered ample sediment quantities to the continental slope, giving rise to an expanded sedimentary sequence [Forsberg et al., 2007].

Supplementary Figure 3 shows the seasonal patterns for precipitation and sea surface salinity in the study region. Precipitation data is an average from 1948-2009 from NOAA Earth System Research Laboratory (ESRL). Precipitation maxima occur during Jul-Sep, and highest rainfall areas are located in the western and northeastern part of the Indian peninsula associated with the orographic effects of the Western Ghats and the Himalayan plateau respectively. Another region of high rainfall occurs in northeastern India and extends westward into the head of the Bay of Bengal, defining the core monsoon zone [*Gadgil,* 2003]. Salinity fluctuations occur

simultaneously, with the appearance of a coastal freshwater plume fed by Indian rivers during the summer monsoon season and in the northwest margin of the Bay of Bengal. Sea surface salinity is from the Levitus database [*Antonov et al.*, 2006] from IRI/Lamont-Doherty Earth Observatory Climate Data Library. Supplementary Figure 3 also includes the drainage area of the Godavari River in context with climatology.

4. Archaeological evidence for subsistence, settlement and trends in human population in late prehistoric South India.

Archaeological evidence provides a record of past populations and their subsistence strategies [*Hassan*, 1981]. Throughout most of the early and middle Holocene populations in peninsular India (Figure 1a in main text) continued the hunter-gatherer traditions of the Late Pleistocene, characterized by a Mesolithic technology that focused on composite tools using a complex of microlithic artefacts [*Misra*, 2002; *Clarkson et al.,* 2009]. Such societies were predominantly mobile. Ceramics and groundstone tools are generally associated with food-producing societies of the past 5000 years in which population size is expected to have increased and mobility decreased. South India, specifically the Southern Deccan Plateau, has been identified as a region of early cultivation of indigenous Indian millet began around 5000 years ago, while the Northern Deccan provides evidence for early farming based on a mixture of South Indian crops and those introduced from the Indus region, such as wheat and barley [*Fuller*, 2006; 2008; 2011]. Wheat and barley subsequently spread southwards after 4000 years ago. This early farming was focused initially on the drier savannah corridor and some dry deciduous woodland areas down the middle of the Indian peninsula [*Asouti and Fuller,* 2008; *Fuller,* 2011]. The indigenous crops of South India included minor millets as staple cereals, *Brachiaria ramosa* and *Setaria verticillata,* both

C_4 grasses, as well as C_3 legumes *Macrotyloma uniflorum* and *Vigna radiata*. Thus early farming in the Deccan replaced C_4 dominated savannah and adjacent woodland with cultivated flora with a similarly large C_4 component. Later periods saw a broadening of the crop repertoire, much of this involved additional C_4 crops, such as little millet (*Panicum sumatense*) and kodo millet (*Paspalum scrobiculatum*), native to other parts of India, and millets of African origin (*Sorghum, Eleusine, Pennisetum*). The adoption of rice, which is a C3 plant, took place after 1000 BC and was more restricted towards coastal regions and the far south, especially near population centers [*Fuller*, 2006; *Fuller et al.,* 2010]. After 1,500 BC and increasingly over the subsequent 1,000-2,000 years, agricultural settlements encroached into the moister tropical forest zones in the Western Ghats [*Kingwell-Banham and Fuller*, 2011] introducing C_4 anthropogenic vegetation into a zone with naturally higher proportions of C_3 vegetation. In the Eastern Ghats region, which stores most of the C_3 vegetation in the Godavari watershed, smaller scale shifting cultivation was typical until modern times; this type of agriculture replaces forest tracts used temporarily for agriculture with fast growing C_3 forests after abandonment, notably sal (*Shorea robusta*) forests in the east and north with more teak (*Tectona grandis*) towards the west [*Kingwell-Banham and Fuller,* 2011]. Massive and permanent deforestation in the Eastern Ghats took place during British colonial times in the 19th century [*Hill*, 2008], which led to a rapid expansion of the Godavari delta [*Rao et al*., 2005].

It has previously been suggested that the beginnings of agriculture in the Deccan region are associated with the beginnings of a trend towards increasing aridity, and declining monsoons across this region [*Fuller and Korisettar,* 2004; *Fuller,* 2008; 2011]. Given the new palaeoclimatic data reported in this paper, we wanted to consider the archaeological evidence as a proxy for human population and reliability of early agricultural practices to assess any

correlations between major cultural and climatic changes in this region. There have been few systematic studies of prehistoric settlement patterns in south India, all restricted to small regions [e.g. *Paddayya*, 1973; *Venkatasubbaiah,* 1992; *Shinde*, 1998]. Nevertheless available archaeological data provides a record of past human population in the region, biased towards sedentary agriculturalists who would have lived at higher population densities than hunters or shifting cultivators [cf. Kingwell-Banham and Fuller 2011]. We therefore compiled counts of known archaeological sites from the third millennium BC (5,000 BP) through the first millennium BC (2,000 BP) for the states of Andhra Pradesh, Karnataka, and Maharashtra (Supplementary Table 2). For sites of the earlier period, referred to the Southern Neolithic in Karanataka and Andhra, and the Deccan Chalcolithic in Maharashtra, we followed the quasi-comprehensive map published in *Asouti and Fuller* [2008] (Supplementary Table 3). For the subsequent Iron Age, also known as the 'Megalithic Period' we used the site counts in *Moorti* [1994] (Supplementary Table 4), which provided a comprehensive compilation at the time of its publication. These data have a number of drawbacks. First, because of the vagaries of archaeological phasing based on material culture, chronological divisions are often potentially finer in periods that have been more heavily sampled, including the upper strata of deeply stratified sites, and archaeological phases are not all of equal length. Second, site numbers cannot be directly computed as population since site sizes may vary and the density of human populations of sites may vary systematically, nevertheless very few sites will represent less population than many sites, especially when difference are in orders of magnitude. Thirdly, the type of sites varies between the earlier Neolithic/Chalcolithic and the later Iron Age periods: in the Iron Age many sites consist of cemeteries, which have been easier to find because of monumental stone superstructures on tombs, whereas in the earlier period all sites represent

occupation sites and burials when they do occur are found within those sites. Our tallies for the Iron Age therefore include both cemeteries (which are likely to have connected to nearby settlements even when these have not been found) and habitation sites, and this may lead to an over estimation (Iron Age versus earlier). Iron Age cemeteries have perhaps been easier to find too, so fieldwork may be biased towards finding these. For these reasons Iron Age numbers may be overestimated relative to earlier site numbers but the differences are so great as to suggest that some change is represented despite this.

An additional approach to estimating relative population sizes across regions is to use summed probability distributions of calibrated radiocarbon dates, which we have attempted here for the earlier Neolithic/Chalcolithic period for the southern and northern Deccan plateau. This approach has been used for example to look at population growth in Britain with the beginnings of agriculture [*Collard et al*., 2010a] and hunter-gatherers population dynamics in north American and northern Europe [e.g. *Shennan and Edinborough,* 2007; *Collard et al*., 2010b). This approach assumes that radiocarbon dates represent a more or less random sample of available archaeological evidence and therefore periods with higher population are more likely to have been dated more times. It also assumed than any regional biases, such as those due to research focuses on particular periods, will be insignificant by comparison to large chronological trends in the data. For south India the total number of radiocarbon dates is quite limited (Supplementary Table 3) by comparison to the thousands of dates in European databases for example. For example a recent study of the Neolithic of South India reports just 116 dates from 23 sites [*Fuller et al*., 2007]. This dataset was used to produce a summed distribution of all radiocarbon dates associated with the Southern Neolithic. In the North Deccan most dates have been associated with particular long excavation projects, mostly conducted in the 1970s and

1980s, and so the total number of dated sites with readily available data is limited to 83 dates and 11 sites [data from: *Possehl and Rissman*, 1992; *Shinde,* 1998]. Radiocarbon dates from the Iron Age are, by contrast, much more limited and dating has often been inferred from grave artefacts. Therefore we have not attempted to include radiocarbon data from this later period. While such data are an imperfect dataset, they still demonstrate that there is an apparent growth in population, which was based on agricultural villages, over the course of the Second Millennium BC, i.e., after 4,000 BP (Supplementary Table 4). Radiocarbon dates were summed with the OxCal 3.10 software [*Bronk Ramsey*, 2001; 2005]. The sums for the North Deccan and South Deccan have been run separately and each is scaled independently as the relative contribution of radiocarbon date contribution to the dataset at any given point in time. For ease of viewing, these two datasets have been plotted along the same time scale with one shown inverted below the timeline in Supplementary Figure 4.

The patterns in these data point to directional increases in archaeological population after 4,000 BP up to ca. 3,300 BP for South India and 3,200 BP for the North Deccan. While the declines after this time are to a large degree a product of the end of respective archaeological phases, it also does appear to represent a period of major social transformation. A great many sites of the Jorwe cultural phase in the North Deccan [*Shinde,* 1998] and at this stage many of the hilltop settlement sites of the Southern Neolithic cease to be occupied at this period [*Fuller et al*., 2007]. While the earliest dates for the Iron Age come from around this period, most of the Iron Age in the North Deccan indicates an eastward shift in settlement distribution to the somewhat wetter subzones of eastern Maharashtra. By contrast in South India there is continuity in the regions that were previously occupied and more regions came to be occupied after Neolithic. Nevertheless, as in the Neolithic period, Iron Age settlement seems to predominantly focus on

savannah and dry-deciduous zone when judged by modern rainfall patterns (Supplementary Table 4). Nevertheless there are local shifts. For example, many more settlements are found on the plains in contrast to predominantly hilltop locations in the Neolithic. These changes with the transition to the Iron Age are increasingly seen as driven by social changes, as opposed to earlier ideas about new immigrants [*Moorti,* 1994; *Fuller et al.,* 2007]. Nevertheless, there is clearly overall increase in agriculture and population in the Deccan as a whole after the 2,000 BP onset of highly arid conditions, which can be contrasted with some other parts of the South Asian subcontinent such as in the Indus valley [*Madella and Fuller,* 2006].

5. Data Analysis

5.1 $\delta^{18}O$ *G. ruber*

G. ruber is abundant in the surface mixed layer (~100m) but its shell growth has been found to be restricted to the top 35 m of water [*Fairbanks et al*., 1982]. In sediment trap studies from the Arabian Sea and the Bay of Bengal, *G. ruber* has been found to be a year-round species with summer peak abundances [*Curry et al*., 1992; *Unger et al*., 2003]. The habitat of this species is ideal to record salinity and SST where and when fluctuations are highest. Our $\delta^{18}O$ *G. ruber* record after 3000 years BP exhibits brief excursions of ca. 0.6 to over 1‰ heavier than the background values (between -2.9 and -2.5 ‰). According to the calcification equation for *G. ruber* [*Mulitza et al*., 2003], the temperature increase of 2.5°C, the maximum Holocene variability in the Arabian Sea (Govil and Naidu, 2010) and Bay of Bengal (Govil and Naidu, 2011), can explain 0.56 ‰ of the amplitude of these positive excursions in $\delta^{18}O$ *ruber*. We have also corrected the raw $\delta^{18}O$ *ruber* data for ice volume effects using a glacio-eustatic sea level record for the Holocene [*Fairbanks*, 1989] and a sea level - $\delta^{18}O$ water relationship of

0.0083‰/m [*Adkins and Schrag*, 2003].

5.2 $\delta^{13}C$ in *n*-alkanoic acids

$\delta^{13}C$ was measured on *n*-alkanoic acids (C_{26}-C_{32}) from 42 sediment samples. All measurements were done in triplicate. Results are plotted on Supplementary Figure 5. The solid line represents the weighted average of $\delta^{13}C$ measurements for *n*-alkanoic acids (C_{26}-C_{32}). This weighted average was calculated by taking into account the concentration of each homologue and its $\delta^{13}C$ value:

$$\text{Wt. Average} = (C_1X_1 + C_2X_2 + \ldots\ldots + C_nX_n) / (C_1 + C_2 + \ldots + C_n)$$

where X is the measured $\delta^{13}C$ average value for a particular *n*-alkanoic acid and C its concentration in the sample.

A previous study [*Chikaraishi et al.*, 2004] measured the $\delta^{13}C$ of the different *n*-alkanoic acids directly extracted from C_3 and C_4 modern plants. From their reported values we extracted 52 measurements for *n*-alkanoic acids of C_3 plants between C_{26} and C_{32} averaging -37.7 ± 1.8 ‰ and 16 measurements of the same compounds in C_4 plants with an average of -21.1 ± 1.4 ‰. Using these values as end members [-37.7 = 0% C_4 plants; -21.1 = 100% C_4], we expressed our $\delta^{13}C$ plant wax values as a percentage of C_4 plants in the Godavari river catchment (Fig 2(e), secondary axis in black). We excluded from our analysis 2 samples measured in the core interval between 2.78 and 2.93 cm depth in core NGHP-16A due to anomalously high woody and charred organic matter visible under microscope as it may represent a direct and/or a redeposition event similar to events that are encountered deeper within core as organic-rich

turbidites.

The measured $\delta^{13}C$ value of a sample can be expressed as a mixture of pure C_3 and C_4 plants. Where (f) is the fraction of C_4 plants, $(1-f)$ the fraction of C_3 plants in the mixture, and f is a number between 0 and 1:

(1) $$\delta^{13}C_{sample} = f \cdot \delta^{13}C_4 + (1-f) \cdot \delta^{13}C_3$$

For simplicity in nomenclature, equation (1) can be written as:

(1.1) $$\delta = f \cdot \delta C_4 + (1-f) \cdot \delta C_3$$

Where δ is the $\delta^{13}C$ value of the sample, f the fraction of C_4 plants, δC_4 the $\delta^{13}C$ value of a pure C_4 plant, and δC_3 the $\delta^{13}C$ value of a pure C_3 plant.

If we rearrange equation (1.1) to clear for f, then the fraction of C_4 plants represented by a single $\delta^{13}C$ value of a sample could be expressed as:

(1.2) $$f = \frac{\delta - \delta C_3}{\delta C_4 - \delta C_3}$$

Using equation (1.2) and the previously calculated end member $\delta^{13}C$ values for C_3 and C_4 plants we estimated the percent of C_4 vegetation coverage in the central Indian peninsula during the Holocene, given that the recovered sediment samples represent an integrated signal of vegetation cover in the Godavari River catchment.

To quantify uncertainties associated with this estimate of C_3 /C_4 ratios based on a simple end-member mixing model we propagate the errors introduced by instrumental uncertainties in the measurement of our samples, and the variability of measured $\delta^{13}C$ values for different species of

C_3 and C_4 plants used to calculate the end-member values. Based on the error propagation equation of *Bevington and Robinson* [1992] the variance (square of the standard deviation, σ) in the estimated fraction of C_4 plants (f) can be expressed as:

$$(2) \qquad \sigma_f{}^2 = \left(\frac{\partial f}{\partial \delta}\sigma_\delta\right)^2 + \left(\frac{\partial f}{\partial \delta C_3}\sigma_{\delta C_3}\right)^2 + \left(\frac{\partial f}{\partial \delta C_4}\sigma_{\delta C_4}\right)^2$$

After solving the three partial derivatives of f with respect to the $\delta^{13}C$ values of the sample, and the C_3 and C_4 end-members, equation (2) can be expressed as:

$$(2.1) \qquad \sigma_f{}^2 = \frac{f^2}{(\delta - \delta C_3)^2}\cdot \sigma_\delta{}^2 + \frac{f^2\cdot (f-1)^2}{(\delta - \delta C_3)^2}\cdot \sigma_{\delta C_3}{}^2 + \frac{f^2}{(\delta C_4 - \delta C_3)^2}\cdot \sigma_{\delta C_4}{}^2$$

And further simplified into:

$$(2.2) \qquad \left(\frac{\sigma_f}{f}\right)^2 = \frac{\sigma_\delta{}^2}{(\delta - \delta C_3)^2} + (f-1)^2\cdot \frac{\sigma_{\delta C_3}{}^2}{(\delta - \delta C_3)^2} + \frac{\sigma_{\delta C_4}{}^2}{(\delta C_4 - \delta C_3)^2}$$

Solving for the standard deviation in the calculated fraction of C_4 plants (σ_f) provides a way to quantify the propagated error in the application of the mixing model to estimate changes in vegetation cover:

$$(2.3) \qquad \sigma_f = \sqrt{\left[\frac{\sigma_\delta{}^2}{(\delta - \delta C_3)^2} + (f-1)^2\cdot \frac{\sigma_{\delta C_3}{}^2}{(\delta - \delta C_3)^2} + \frac{\sigma_{\delta C_4}{}^2}{(\delta C_4 - \delta C_3)^2}\right]}\cdot f$$

After solving equation (2.3) for all measured samples in this study, the maximum error in the calculation of the fraction of C_4 plant cover (f) is estimated to be 0.066 and the minimum 0.062 with an average of 0.063. The propagated error estimate for f (fraction of C_4 plants) would correspond to one standard deviation (σ), assuming no correlation between the errors in the different pools of $\delta^{13}C$ measurements (sedimentary plant waxes, C_3 plants, C_4 plants). The calculated propagated error implies an uncertainty of ± 6.3% in the estimation of percent C_4 plant cover. For comparison, the magnitude of the estimated changes in vegetation cover from mid Holocene to late Holocene is ~30%.

The main contributor to error in this mixing model is the variability in the end-members $\delta^{13}C$ values. However, changes in plant biosynthesis in a stressed ecosystem are still poorly constrained. As more studies on plant biosynthesis become available and the survey for compound specific isotopic measurements of plant species diversifies, we will be able to better constrain the end-member values and decrease the uncertainty of the mixing model.

Supplementary Table 1. Radiocarbon ages for mixed planktonic foraminifera and corresponding calendar age. Calendar ages were derived using the CALIB 6.0 radiocarbon calibration program (http://radiocarbon.pa.qub.ac.uk/calib) using the calibration data set Marine09. The standard marine reservoir correction was applied.

NOSAMS #	Depth (cm)	Raw ^{14}C Age		Error	Calibrated Age (yrBP)		1σ error
63284	0-2	155	±	55	0	±	0
85606	62-64	815	±	30	460	±	27
79575	140-142	1,520	±	30	1,082	±	50
63285	280-282	2,160	±	40	1,704	±	4
65825	400-402	3,120	±	35	2,895	±	54
84036	460-462	3,820	±	30	3,769	±	52
80683	520-522	4,580	±	35	4,809	±	39
63286	600-602	5,610	±	50	5,996	±	68
63287	700-702	7,890	±	50	8,356	±	46
63287	800-802	10,350	±	75	11,319	±	99
63289	850-852	33,000	±	240	25,420	±	257

Supplementary Table 2. Tally of archaeological sites by period and region. For the period 3,200-2,200 BP, site counts are taken from *Moorti* [1994].

Period (BP)	5000-4500	4500-4000	4000-3400	3200-2200
S.Deccan	3	8	180	91
N.Deccan	0	15	75	965
total	3	23	255	1056

Supplementary Table 3. A tally of sites and radiocarbon dates for Neolithic/Chalcolithic Indian peninsula (Deccan Plateau). To fill out the cultural periods of the Northern Deccan some sites from Madhya Pradesh have been included. Citations provided here include secondary compilations of earlier data.

State	Site	Number of dates	Source
Maharashtra	Apegaon	3	Shinde 1994
Maharashtra	Chandoli	2	Shinde 1994
Maharashtra	Daimabad	18	Shinde 1994
Maharashtra	Inamgaon	37	Shinde 1994
Maharashtra	Kaothe	1	Shinde 1994
Maharashtra	Songaon	5	Shinde 1994
Madhya Pradesh	Dangwada	6	Sharma and Misra 2003
Madhya Pradesh	Eran	11	Sharma and Misra 2003
Madhya Pradesh	Kayatha	22	Sharma and Misra 2003
Madhya Pradesh	Navdatoli	8	Sharma and Misra 2003
Karnataka	Budihal	15	Fuller et al 2007
Karnataka	Sannarachamma (Sanganakallu)	13	Fuller et al 2007
Karnataka	Hiregudda	13	Fuller et al 2007
Karnataka	Hallur	11	Fuller et al 2007
Karnataka	Tekkalakota	8	Fuller et al 2007
Karnataka	Piklihal	8	Fuller et al 2007
Karnataka	Watgal	7	Fuller et al 2007
Andhra Pradesh	Veerapuram	5	Fuller et al 2007
Andhra Pradesh	Ramapuram	5	Fuller et al 2007
Karnataka	Birappa	5	Fuller et al 2007
Andhra Pradesh	Hanumantaraopeta	4	Fuller et al 2007
Andhra Pradesh	Utnur	3	Fuller et al 2007
Andhra Pradesh	Sanyasula Gavi	3	Fuller et al 2007
Karnataka	Terdal	2	Fuller et al 2007
Karnataka	Banahalli	2	Fuller et al 2007
Karnataka	Narsipur	2	Fuller et al 2007
Andhra Pradesh	Palavoy	2	Fuller et al 2007
Andhra Pradesh	Velpumudugu	2	Fuller et al 2007
Karnataka	Kurugodu	1	Fuller et al 2007
Karnataka	Kodekal	1	Fuller et al 2007
Andhra Pradesh	Biljapalle	1	Fuller et al 2007
Andhra Pradesh	Hattibelagallu,	1	Fuller et al 2007

Supplementary Table 4. A tally of Iron Age ("megalithic") sites in South India in relation to rainfall zone [*Moorti*, 1994]. Note that this tally includes sites from Kerala and Tamil Nadu, and therefore has greater total number than Table D1, which considers a more restricted region.

Rainfall zone (modern)	Habitation site	Habitation & burial site	Burial site	Total
<600 mm	19	96	201	316
600-1000 mm	61	103	559	723
1000-1500 mm	19	57	343	419
1500-3000 mm		2	188	190
>3000 mm		1	94	95

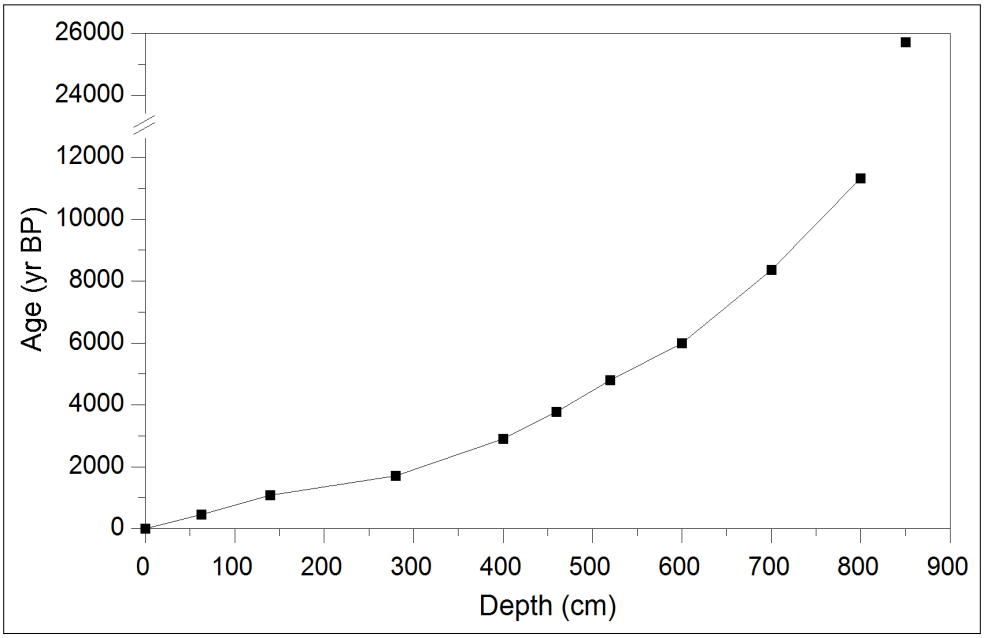

Supplementary Figure 1. Age-depth relationship for core NGHP-16A. Error bars (Supplementary Table 1) are smaller than symbols denoting data points (black squares).

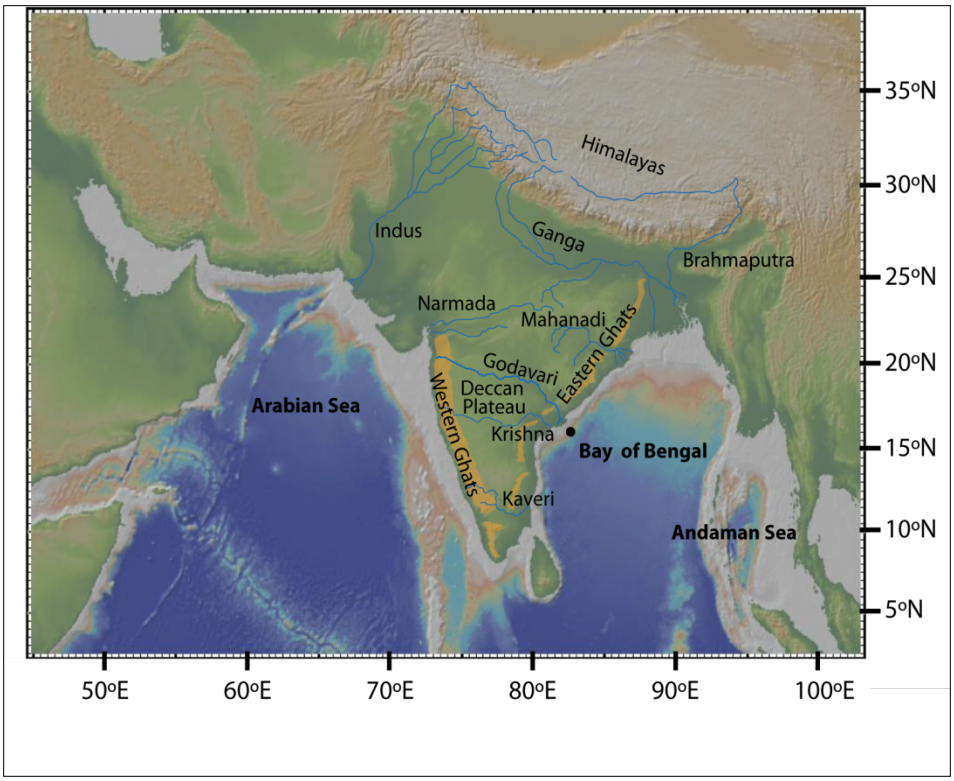

Supplementary Figure 2. Geography of the Indian Peninsula. Schematic outline of the Western and Eastern Ghats are shown in orange. NGHP-16A core location indicated by black dot. Bathymetry of Indian Ocean and Asian topography is from GMRT database [*Ryan et al*., 2009].

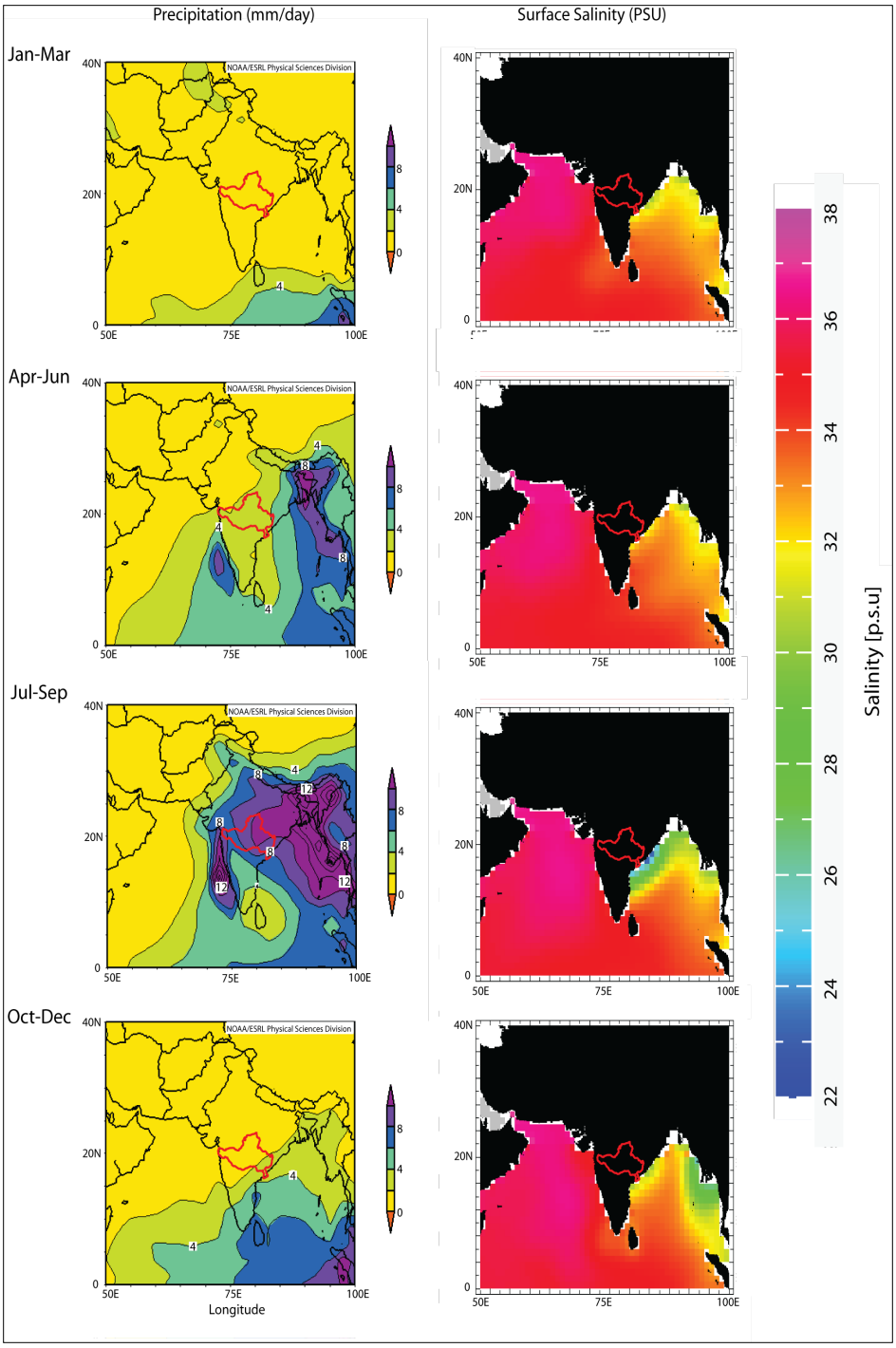

Supplementary Figure 3. Hydro-climatology of the Indian peninsula and Bay of Bengal. Panels on the left are precipitation average 1948-2009 from NOAA/ESRL GPCP http://www.esrl.noaa.gov/psd/data/gridded/data.gpcp.html. Panels on the right are sea surface salinity [*Antonov et al.*, 2006]. Godavari River catchment outline in red.

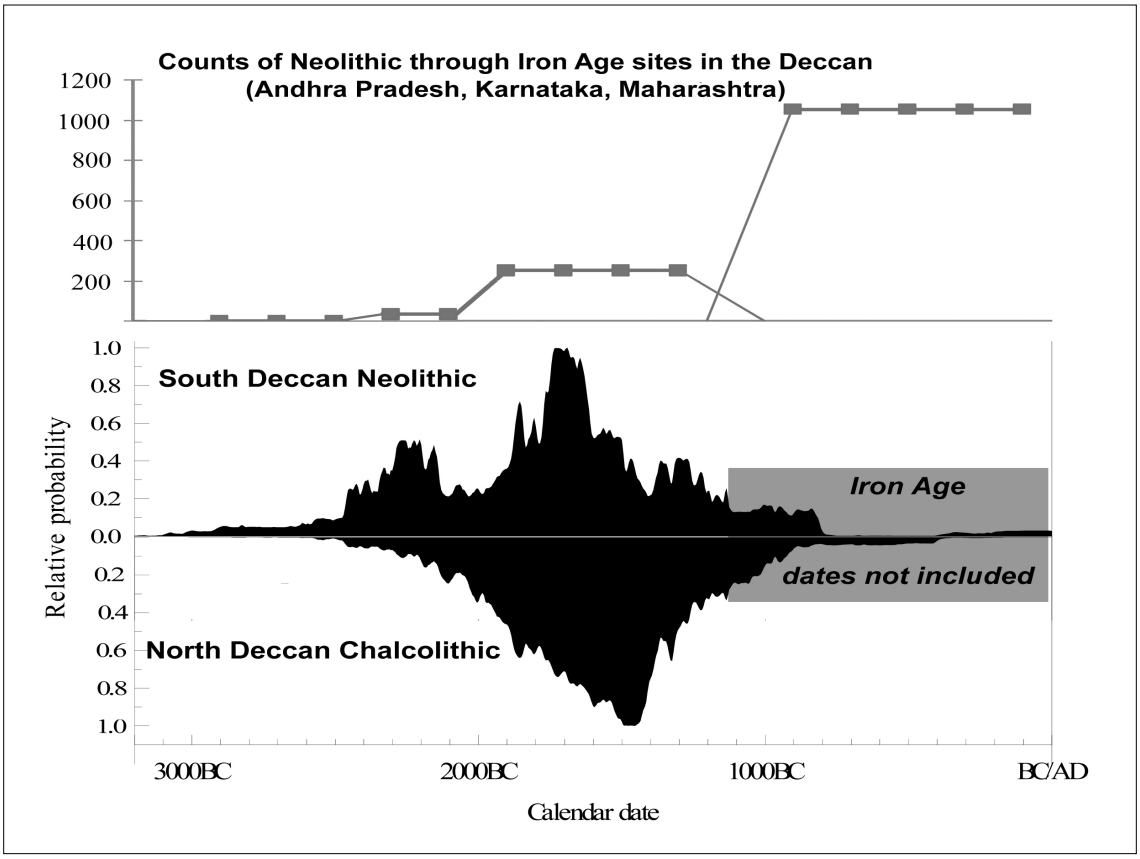

Supplementary Figure 4. Proxies for population dynamics in peninsular India between 5,000 and 2,000 years ago. The top chart is a count of known archaeological sites that plausibly relate to the farming societies. The lower chart represents the summed probability of the calibrated radiocarbon ages for the Neolithic/Chalcolithic, with the North and South Deccan as separate plots on the same time scale.

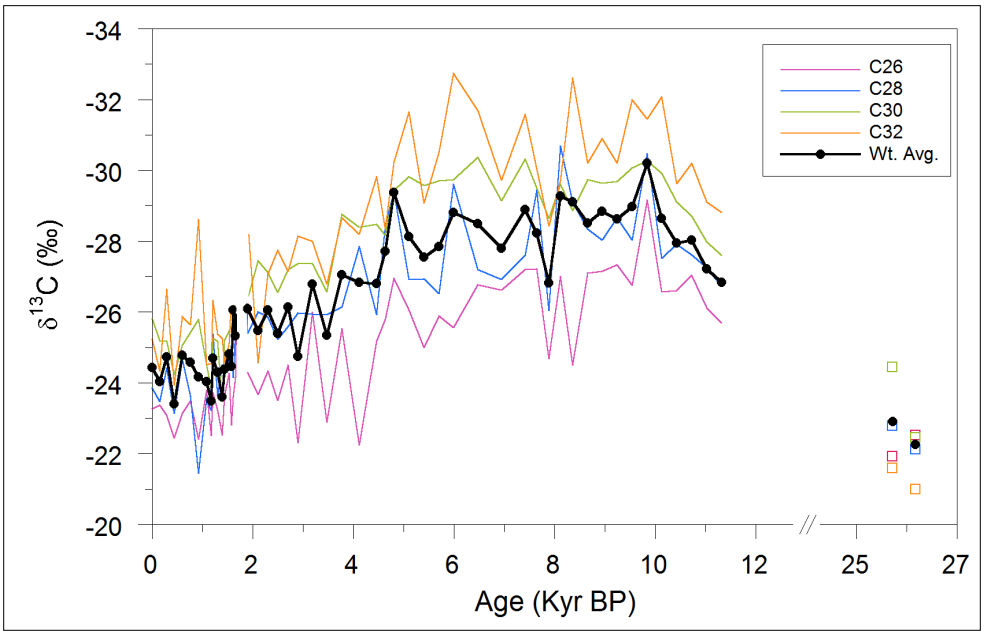

Supplementary Figure 5. $\delta^{13}C$ values of *n*-alkanoic acids from core NGHP-16A. The black curve is the weighted average, and solid black circles representing data points. Colored curves are the different homologues (C_{26}-C_{32}). Open squares represent homologues of the last glacial period samples according to the same color conventions. Changes in $\delta^{13}C$ represent integrated rainfall variations in the Godavari basin expressed as changes in the relative proportions of C_3 vs C_4 plant cover.

References

Adkins, J. F., and D. P. Schrag (2003), Reconstructing Last Glacial Maximum bottom water salinities from deep-sea sediment pore fluid profiles, *Earth and Planetary Science Letters*, *216*(1-2), 109-123.

Antonov, J.I., R.A. Locarnini, T.P. Boyer, A.V. Mishonov, and H.E. Garcia (2006), Sea Surface Salinity, in *World Ocean Atlas 2005*, *Vol. 2: Salinity,* edited by S. Levitus, Ed., NOAA, Washington, D.C.

Asouti, E. and D.Q. Fuller, (2008) *Trees and Woodlands in South India. Archaeological Perspectives,* Left Coast Press, Walnut Creek, Calif.

Bevington, P.R. and D.K. Robinson, (1992) *Data Reduction and Error Analysis for the Physical Sciences,2nd edition,* WCB/McGraw-Hill, USA.

Bikshamaiah, G., and V. Subramanian (1980), Chemical and sediment mass-transfer in the Godavari River Basin in India, *Journal of Hydrology*, *46*(3-4), 331-342.

Bronk Ramsey, C. (2001), Development of the radiocarbon calibration program OxCal, *Radiocarbon,* 43(2A), 355-63.

Bronk Ramsey, C. (2005), OxCal version 3.10. Computer Program. Available at: http://c14.arch.oxoac.uk/.

Chikaraishi, Y., H. Naraoka, and S. R. Poulson (2004), Hydrogen and carbon isotopic fractionations of lipid biosynthesis among terrestrial (C3, C4 and CAM) and aquatic plants, *Phytochemistry*, *65*(10), 1369-1381.

Clarkson, C., et al. (2009), The oldest and longest enduring microlithic sequence in India: 35 000

years of modern human occupation and change at the Jwalapuram Locality 9 rockshelter, *Antiquity*, *83*(320), 326-348.

Collard, M., B. Buchanan, M. J. Hamilton, and M. J. O'Brien (2010a), Spatiotemporal dynamics of the Clovis-Folsom transition, *Journal of Archaeological Science*, *37*(10), 2513-2519.

Collard, M., K. Edinborough, S. Shennan, and M. G. Thomas (2010b), Radiocarbon evidence indicates that migrants introduced farming to Britain, *Journal of Archaeological Science*, *37*(4), 866-870.

Curry, W. B., D. R. Ostermann, M. V. S. Guptha, and V. Ittekkot (1992), Foraminiferal production and mosoonal upwelling in the Arabian Sea: evidence from sediment trap, in *Upwelling Systems: Evolution since the Early Miocene*, edited by E. A. Se, pp. 93-106, Geological Society Special Publication.

Dutta, K., R. Bhushan and B.L. Somayajulu (2001), Delta R correction values for the northern Indian Ocean, *Radiocarbon,* 43, 483-488.

Fairbanks, R. G. (1989), A 17,000-year glacio-eustatic sea-level record - influence of glacial melting rates on the Younger Dryas event and deep-ocean circulation, *Nature*, *342*(6250), 637-642.

Fairbanks, R. G., M. Sverdlove, R. Free, P. H. Wiebe, and A. W. H. Be (1982), Vertical-distribution and isotopic fractionation of living planktonic-foraminifera from the Panama Basin, *Nature*, *298*(5877), 841-844.

Forsberg, C. F., A. Solheim, T.J., Kvalstad, R. Vaidya, and S. Mohanty (2007), Slope instability and mass transport deposits on the Godavari river delta, east Indian margin from a regional geological perspective, *Submarine Mass Movements and Their Consequences 27*, 19-27.

Fuller, D.Q. (2006), Agricultural Origins and Frontiers in South Asia: A Working Synthesis. *Journal of World Prehistory,* 20, 1-86.

Fuller, D.Q. (2008). Asia, South: Neolithic Cultures*,* in *Encyclopedia of Archaeology,* edited by D. Pearsall, pp.756-768, Elsevier, Amsterdam.

Fuller, D.Q. (2011), Finding Plant Domestication in the Indian Subcontinent. *Current Anthropology*, 52(S4), S347-S362

Fuller, D.Q. and R. Korisettar, (2004), The Vegetational Context of Early Agriculture in South India, *Man and Environment XXIX*(1)*,* 7-27.

Fuller, D. Q., N. Boivin, and R. Korisettar (2007), Dating the Neolithic of South India: new radiometric evidence for key economic, social and ritual transformations, *Antiquity*, *81*(313), 755-778.

Gadgil, S. (2003), The Indian monsoon and its variability, *Annual Review of Earth and Planetary Sciences*, *31*, 429-467.

Govil, P., and P. D. Naidu (2010), Evaporation-precipitation changes in the eastern Arabian Sea for the last 68 ka: Implications on monsoon variability, *Paleoceanography*, *25*.

Govil, P., and P. D. Naidu (2011), Variations of Indian monsoon precipitation during the last 32 kyr reflected in the surface hydrography of the Western Bay of Bengal, *Quaternary Science Reviews*, 30, 3871-3879.

Gunnell, Y., K. Anupama, and B. Sultan (2007), Response of the South Indian runoff-harvesting civilization to northeast monsoon rainfall variability during the last 2000 years: instrumental records and indirect evidence, *Holocene*, *17*(2), 207-215.

Hassan, F.A. (1981), *Demographic Archaeology,* Academic Press, New York.

Hill, C.V., 2008, South Asia: An Environmental History, ABC-CLIO Press, 329 p.

Kingwell-Banham E. and D.Q. Fuller (2011), Shifting cultivators in South Asia: expansion, marginalisation and specialisaton over the long term. *Quaternary International* [on-line/in press]: DOI: 10.1016/j.quaint.2011.05.025.

Madella, M., and D. Q. Fuller (2006), Palaeoecology and the Harappan Civilisation of South Asia: a reconsideration, *Quaternary Science Reviews*, *25*(11-12), 1283-1301.

Misra, V.N. (2002), Mesolithic culture in India, in *Mesolithic India,* edited by V.N. Misra and J.N. Pal, pp. 1-66, Department of Ancient History, Culture and Archaeology, University of Allahbad, Allahbad, India.

Moorti, U.S. (1994), *Megalithic Culture of South India. Socio-economic Perspectives,* Ganga Kaveri Publishing House, Varanasi.

Mulitza, S., D. Boltovskoy, B. Donner, H. Meggers, A. Paul, and G. Wefer (2003), Temperature: delta O-18 relationships of planktonic foraminifera collected from surface waters, *Palaeogeography Palaeoclimatology Palaeoecology*, *202*(1-2), 143-152.

Paddayya K. (1973), *Investigations into the Neolithic Culture of the Shorapur Doab, South India,* Brill, Leiden.

Possehl, G.L. and P. Rissman (1992). The chronology of prehistoric India from earliest times to the Iron Age, in *Chronologies in old world archaeology, edited by* R.W. Ehrich, pp. 1, 465–490; 462, 447–474, University of Chicago Press, Chicago.

Rao, K.N., Sadakata, N., Malini, B.H., Takayasu, K., 2005, Sedimentation processes and

asymmetric development of the Godavari delta, India, in River Deltas: Concepts, Models, and Examples, edited by L. Giosan, and J.P. Bhattacharya, pp. 435-452, SEPM Special Publication 83.

Reimer, P. J., et al. (2009), INTCAL09 and MARINE09 radiocarbon age calibration curves, 0-50,000 years cal BP, *Radiocarbon*, *51*(4), 1111-1150.

Ryan, W. B. F., et al. (2009), Global Multi-Resolution Topography synthesis, *Geochemistry Geophysics Geosystems*, *10*.

Sharma R.K. and O.P. Misra (2003), *Archaeological Excavations in Central India (Madhya Pradesh and Chhattisgarh),* Mittal Publications, New Delhi.

Shennan, S., and K. Edinborough (2007), Prehistoric population history: from the late glacial to the late neolithic in central and northern Europe, *Journal of Archaeological Science*, *34*(8), 1339-1345.

Sridhar, P. N., M. M. Ali, P. Vethamony, M. T. Babu, I. V. Ramana, and S. Jayakumar (2008), Seasonal Occurrence of Unique Sediment Plume in the Bay of Bengal, *EOS Trans. AGU 89*, 22-23.

Shinde, V.S. (1994), The Deccan Chalcolithic: a recent perspective, *Man and Environment* 19, 1-2.

Shinde, V.S. (1998), *Early Settlements in the Central Tapi Basin,* Munshiram Manoharlal, New Delhi.

Southon, J., M. Kashgarian, M. Fontugne, B. Metivier, and W. W. S. Yim (2002), Marine reservoir corrections for the Indian Ocean and southeast Asia, *Radiocarbon*, *44*(1), 167-180.

Stuiver, M., and P. J. Reimer (1993), Extended C-14 data-base and revised calib 3.0 C-14 age calibration program, *Radiocarbon*, *35*(1), 215-230.

Unger, D., V. Ittekkot, P. Schafer, J. Tiemann, and S. Reschke (2003), Seasonality and interannual variability of particle fluxes to the deep Bay of Bengal: influence of riverine input and oceanographic processes, *Deep-Sea Research Part II-Topical Studies in Oceanography*, *50*(5), 897-923.

Venkattasubbaiah, P.C. (1992), Protohistoric investigation in the Central Pennar Basin, Cuddapah, Andhra Pradesh, PhD Thesis, University of Poona, Pune, India.

Washington, H. S. (1922), Deccan traps and other plateau basalts, *Bulletin of the Geological Society of America*, *33*, 765-803.